THERMAL CHARACTERIZATION OF CORK- AND CERAMICS-BASED TPS IN DLRS ARC-HEATED WIND TUNNEL L2K

Christian Hantz[1], Ansgar Marwege[1], Sofia Paixao[2], Luca Celotti[3], Maria Wiśniewska[4]

[1] German Aerospace Center (DLR), Institute of Aerodynamics and Flow Technology
Supersonic and Hypersonic Technologies Department, Linder Hoehe, 51147 Cologne, Germany
christian.hantz@dlr.de

[2] Amorim Cork Composites
Rua Comendador Américo Ferreira Amorim, 260, 4535-186 Mozelos, Santa Maria da Feira, Portugal

[3] Azimut Space GmbH, Carl-Scheele-Strasse 14, 12489 Berlin, Germany

[4] Łukasiewicz Research Network – Poznań Institute of Technology
6 Ewarysta Estkowskiego St., 61-755, Poznan, Poland

ABSTRACT

Within the RETALT project, multiple Thermal Protection System (TPS) materials have been tested, using DLR´s arc heated facility L2K in Cologne, Germany. The high enthalpy flow was used to simulate the aerothermal heating during reentry of the 1st stage of the RETALT 1 launcher.

In total, 21 samples of five materials in stagnation point configuration have been tested, having two ablative cork materials and three high temperature ceramics. The cork materials by Amorim Cork Composites featured an existing material (P50) and a newly developed, trowelable cork based TPS. The ceramics were provided in cooperation with the LightCoce project.

The samples were exposed to cold wall heat fluxes in the range of 200 to 800 kW/m². In addition to tests with only one heat exposure, some samples were tested 3 times at the same cold wall heat flux and same total test time, named cycle tests. Those cycle tests are intended to yield more information on a possible reuse of the materials. Surface recession and mass change is measured.

Index Terms— *TPS, reusable launch vehicle, cork ablator, RETALT, LightCoce*

1. INTRODUCTION

The RETALT (Retro Propulsion Assisted Landing Technologies) project investigates key technologies for the reusability of Vertical Take-off Vertical Landing launcher configurations [1]. They are decelerated and landed with the aid of retro propulsion, i.e. firing the engines against the flight direction. The first stage of the RETALT1 configuration, representing a heavy launcher, requires a Thermal Protection System (TPS) for the base area during reentry and landing. For this task, a newly developed and trowelable cork based TPS is foreseen.

This paper describes and summarizes the thermal qualification tests conducted on the different TPS materials tested and the comparison thereof.

TPS is of crucial importance to protect the launcher, especially the fins and base area, from the high thermal loads during reentry, descent and landing. This paper features the characterization of different TPS solutions for the base area, which are subsequently tested and analyzed. The newly developed cork based TPS is compared to an existing conventional cork TPS. Furthermore, three different high temperature ceramics are also considered in cooperation with the LightCoce project [2] and used for an additional comparison. While the cork material is designed to function as ablative protection, the key-characteristic of the ceramic materials is the high temperature resistance and therefore the expected re-usability.

The materials were tested in the arc heated facility “L2K” at DLR´s Supersonic and Hypersonic Technologies Department in Cologne. The samples were exposed to cold wall heat fluxes in the range of 200 to 800 kW/m².

In addition to the tests with only one heat exposure, some samples were tested 3 times at the same cold wall heat flux, namely cycle tests. Thus, the cycle and non-cycle tests can be evaluated by themselves and in relation to each other, as they had the same total exposure time and the same cold wall heat flux. The cycle tests are intended to yield more information on a possible reuse of the materials.

The samples were analyzed in terms of their weight and shape before and after each test. The surface geometry was measured with a 3D-profilometer that provides height information for every point of the sample with an accuracy in the micrometer range. Through this, different levels of surface regression were observed for the ablative TPS, but also for the ceramics TPS.

The paper is laid out as follows: First, the trajectory for the definition of the tested heat loads is describe. Then, the test setup, sample design, material properties and test conditions are described, followed by the discussion of results obtained in the test series. A summary and outlook concludes the paper.

2. TRAJECTORY AND HEAT LOADS

The reference mission for the RETALT 1 configuration is based on a re-entry trajectory as shown in Figure 1, entering the atmosphere

from 100 km with an entry velocity of around 2200 km/s which results in peak heat fluxes of around 280 kW/m² (baseplate, 340 sec).

Results of the Aerodynamic Database (ATDB) [6] were taken to compute the heat flux and heat load values, via simple energy formulations, yielding the temperature profile over time. For the simulation, the baseplate heat fluxes were averaged and projected onto a thin TPS layer (5mm), neglecting other effects like heat conduction, pyrolysis or material recession. The results for TPS05 can be seen in Figure 2, showing the heat flux at every instance of time.

This trajectory and the associated aerothermal loads define the conditions that were targeted in the wind tunnel investigations.

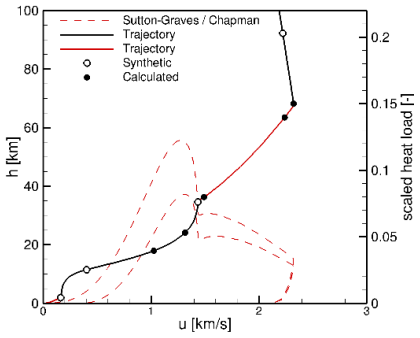

Figure 1: RETALT 1 Descent Trajectory [6]

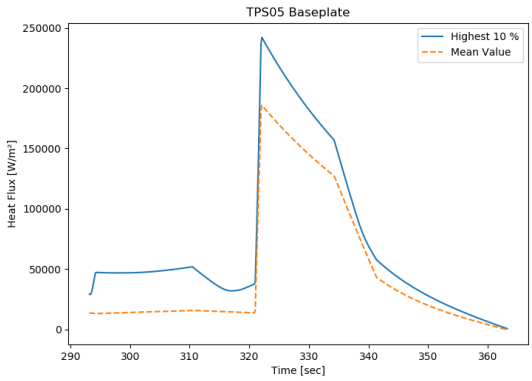

Figure 2: RETALT 1 Descent Heat fluxes for TPS05 on the Baseplate

3. TEST SETUP

The arc-heated facility L2K of DLR Cologne uses a Huels type arc heater with a maximum electrical power of 1.4 MW to energize the working gas to high enthalpy conditions and thus achieves cold wall heat flux rates up to 3 MW/m². Convergent-divergent nozzles with exit diameters of 50 mm, 100 mm or 200 mm, having a conical shape with a half angle of 12°, can be mounted based on the required heat fluxes. The resulting homogeneous hypersonic flow field allows testing of Models with a size of up to 150 mm (W) x 250 mm (L) x 70 mm (H). Furthermore, the L2K can be operated on different gasses, allowing not only to simulate Earth atmosphere, but also e.g. of Mars or Titan. A more detailed description of the facilities is given in [3], [4] and [5].

For the current test series, the L2K was used with the 100 mm and 200 mm nozzle configuration, depending on the design cold wall heat flux. Air was used as working gas for all tests.

4. MATERIALS AND SAMPLE DESIGN

All tests were performed with cylindrical samples with 50 mm diameter. The outer geometry of the samples is equal for all cork's samples. The ceramics samples have no rounded edges and defer in the length due to manufacturing constraints.

4.1. Cork

For the P50 material, the samples were made of a solid block with a thickness of 40 mm. The TPS05 material required multiple curing procedures and exhibited several layers therefore. Due to the low thermal conductivity of both materials, rather low temperatures were expected at the bonding interface to the metallic sample holder, thus, the sample holder was glued directly to the back surface of the sample. The geometry of the cork samples is shown in Figure 3. Photographs of the front surface and general layout of P50 and TPS05 sample are shown in Figure 4 and Figure 5. Four out of five(P50) and six (TPS05) cork samples were instrumented, each with four type K thermocouples. One(P50) and two (TPS05) samples were intended for cycle tests and did not have holes for thermal probes. The material properties of the cork materials are summarized in Table 1.

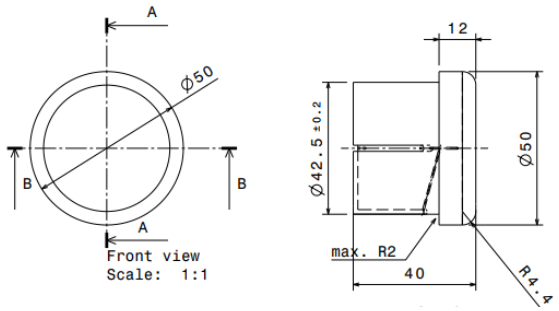

Figure 3: Geometry Cork samples

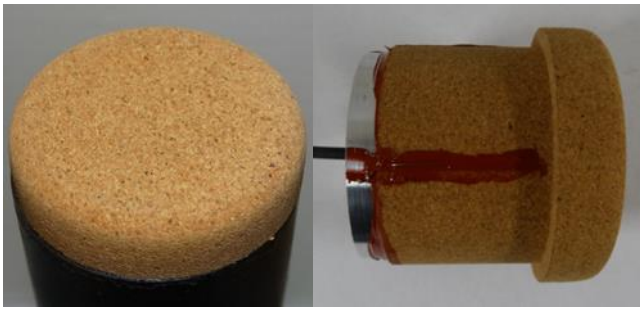

Figure 4: P50 cork sample, front (integrated into test mount) and side view (instrumented, with sample holder plate mounted to the back surface)

Figure 5: TPS05 cork sample, front and side view (instrumented, with sample holder plate mounted to the back surface)

Table 1: Material properties of the tested cork materials

Property (unburned)	P50	TPS05	Unit
Density	0.461	0.715	$\frac{g}{cm^3}$
Thermal Conductivity	0.062 (25°C) 0.080 (200°C)	0.251 (25°C) 0.123 (200°C)	$\frac{W}{m\,K}$
Specific Heat Capacity	1610 (25°C) 2304 (200°C)	2548 (25°C) 1935 (200°C)	$\frac{kJ}{kg\,K}$

4.2. Ceramics

For ceramics, very high temperatures were predicted at the back surface of the samples which are also shorter in length compared to the cork ones, resulting in the need for an alternative mounting concept. The samples were fixed close to the front of the sample holder by short pins, preventing the sample from moving out of the holder. Additionally, there was a need for an insulator between the sample back plane and the rear metallic part of the sample holder. This insulator was made out of alumina wool (RATH, Altraform KVS 185/400), pressed against the sample by a spring, which in turn keeps the fixation pins in place.

Photographs showing the surface and layout of the three ceramic sample types are shown in Figure 6, Figure 7 and Figure 8. The thermocouple inserts were fixed by a Kapton tape, partially resistant to high temperatures. The material properties of the ceramics are summarized in Table 2.

Figure 6: 3YSZ-10vol.%MWCNTs Ceramic side view (fixation pin hole visible)

Figure 7: ZrB_2-40vol.%HfB_2-20vol.%SiC Ceramic side view (fixation pin hole visible)

Figure 8: Ti_3AlC_2 Ceramic top and side view (fixation pin and mounting shell visible)

Table 2: Material properties of the tested ceramics

Property	3YSZ-10vol.%MWCNTs	Ti_3AlC_2	ZrB_2-40vol.%HfB_2-20vol.%SiC	Unit
Density	~ 5.3	~ 4.6	~ 7	$\frac{g}{cm^3}$
Thermal Conductivity	~ 2.5	< 20	~75 (25°C)	$\frac{W}{m\,K}$

5. TEST AND MEASUREMENT SETUP

5.1. Sample Instrumentation

All instrumented cork samples were equipped each with 4 thermocouples of Type K. Three of them were not located along the centerline but at a distance of about 1 mm from the centerline in two perpendicular planes, while the last one was mounted in the centerline from the rear. The distribution was chosen to maximize the distance in between the thermocouples and to minimize the measurement error. Besides the different thermal conductivities of the materials and corresponding differences in expected temperature distributions within the samples, integration depths stayed constant for all materials, allowing a comparison of the test results between cork and ceramics. The distance of the thermocouples is 6, 12, 18 and 36 mm from the frontal surface.

The samples of the three different ceramics were equipped each with one thermocouples of type K in general, only the highest heat flux condition featured two thermocouples, both mounted from the backside. While there is one centered hole, the second one was attached and fixed to the rear surface by a heat resistant tape (Kapton Tape).

Prior to the test campaign, the instrumented cork samples were x-rayed by the Institute for Materials Science at DLR to verify the integration depth of the thermocouples. Figure 9 shows an example x-ray image showing the thermocouple locations. It should be noted that in some ceramic tests with 600 or 800 kW/m² the maximum temperatures of the thermocouples, up to about 1300° C for type K, were significantly exceeded and the accuracy of the measurement after this overshoot cannot be guaranteed anymore.

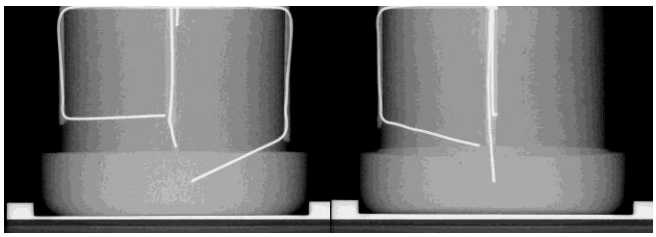

Figure 9: Example x-ray image of sample P50-2 showing thermocouples K1, K3 in one plane (left image) and K2 in the perpendicular plane (right image), while K4 is in the plane's intersection and centered at the top.

5.2. Optical Setup

The thermal response of the samples was mainly characterized by measurements of the surface temperature by two pyrometers, a spectral pyrometer and a two-color pyrometer. The main properties of the pyrometers, including measurement range and sensitive wavelength, are listed in Table 1. For the test campaign, an emissivity value of 1.0 was set for the spectral pyrometer P1. The measurement point of the pyrometers was aligned to the center of the samples in such a way that best possible front view could be achieved.

Table 3: Specifications of pyrometers used in the test campaign

Manufacturer	Model	Mode of operation	Range [°C]	Sensitive wavelength [µm]
Dr. Maurer	KTR 1485	Spectral pyrometer	700 – 3500	0.85 – 1.1
Dr. Maurer	QKTR D 1485-1	Two-color pyrometer	600 – 1600	0.85 – 1.1 0.95 – 1.1
Optris	Optris Pi 1M	IR Camera	500 – 1800	0.85 – 1.1

5.3. Weight Measurements

Weight measurements were done with a Sartorius MC1 LC 1200S, having a tolerance of 5 milligram and a range of 1200 g.

5.4. Recession Measurements

For recession measurements the 3D profiling microscope VR-5000 Series is used. Using a high-intensity LED light and 4-megapixel monochrome CMOS allows to create edge-projection images in one shot.

6. TEST MATRIX

All tests were carried out as stagnation point measurements. The experiments featured two different test types: Regular tests with instrumented samples, exposed only once to the heat loads, and non-instrumented samples, exposed three times but with the same total test time. Latter ones are called "cycle tests".

For both cork materials 4 samples were instrumented and one (P50)/ two (TPS05) were non-instrumented samples (without holes for thermocouples) for the cycle test. All four ceramic samples of the three materials had a hole for a thermocouple, which was not used/ instrumented during the cycle test.

The cork group was tested at cold wall heat fluxes of 200, 400 and 600 kW/m², whereas the cycle tests were performed for 200 kW/m² (both) and 400 kW/m² (TPS05 only). The ceramic group was tested at cold wall heat fluxes of 200, 600 and 800 kW/m², whereas the cycle tests useed the highest heat flux in that group of 800 kW/m².

The test duration was decreased by the factor of the increase of the heat load. Hence, 1/2 from FC 200 to FC 400, and 1/3 from FC 200 to FC 600. As mentioned, the cycle tests had the same total test time, but separated into 3 runs. Thus, all cork samples with the flow condition FC 200 were tested for 180 seconds in total, for FC 400 90 seconds and for FC 600 60 seconds.

For the ceramics, all test times (FC 200, 600, 800) were 240 seconds. Thus, the cycle tests are run 3 times with 80 seconds each. The test times were increased in comparison to the cork samples in order to be able to observe a change and it was kept constant for all flow conditions, to compare the heat flux effects more directly; especially, since the ceramics are no ablators and hence were expected to experience less changes.

7. TEST CONDITIONS

As mentioned in the previous section, the tests consisted of four different design cold wall heat fluxes, namely 200, 400, 600 and 800 kW/m². Each test featured a high-enthalpy flow condition with the goal to apply high and defined heat loads onto the sample. To vary the heat loads, different wind tunnel settings in terms of pressure and arc heater settings were required. For the highest heat load of 800 kW/m², the nozzle had to be changed. The used flow conditions and measured cold wall heat fluxes are listed in Table 4.

Table 4: Nominal test conditions

Test condition	Unit	FC 200	FC 400	FC 600	FC 800
Wind tunnel	[-]	L2K			
Design CWHF	[kW/m²]	200	400	600	800
Operating Gas	-	Air			
Gas mass flow rate#	[g/s]	50			
Distance to nozzle exit#	[mm]	200			
Diameter of nozzle throat / exit#	[mm]	29/ 200		29/ 100	
Reservoir pressure#	[hPa]	1040	1195	1340	1350
Measured CWHF, rounded (4 mm)+	[kW/m²]	224	405	602	814
Measured CWHF, sharp edge+	[kW/m²]	206	377	572	814
Δ CWHF, rounded to sharp edge	[%]	8	7	5	0

CWHF : Cold Wall Heat Flux, # : controlled, + : measured

8. RESULTS

8.1. Recession – Cork

As stated in the section of 5.4 Recession Measurements, 3D images of the samples are taken to gain height information. The evaluation consists of averaging the height information via 36 diameter lines laid over the circular sample top (see Figure 10), creating 2D data of the height profile (see Figure 11). The averaging takes "left" and "right" sides into account, thus the 2D profile has data on both sides of the central axis.

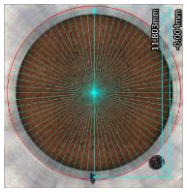

Figure 10: Diameter lines for height averaging

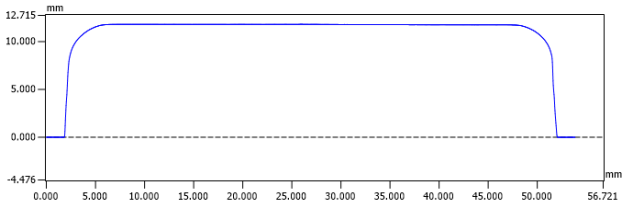

Figure 11: 2D height information results

Due to the fact of being an ablator, cork materials exhibit (much greater) surface recession, whereas the tested ceramics show no or minor recessions. It shall also be noticed, that the TPS05 cork material also shows an increase of the volume, with recession occurring on the sides. A comparison of the pre-test cork shapes showed no discrepancies; hence all samples were identical in terms of their outer shape.

Figure 12 below shows the surface height for all P50 test results. The blue thin double line shows the pre-test shape. The other lines are color graded depending on their heat fluxes (Orange – FC 200, Green – FC 400, Red – FC 600). The dashed lines show the results for the cycle tests.

For all cases, the recession is greater at the outer rim, rounding the samples.

FC 200:

In total, three samples are tested at the FC 200 condition (2 instrumented, 1 cycle). The final height profile of all three is close together. Taking a closer look at the cycle test outcomes, the first cycle outcome shows the smallest recession. The second cycle height lies approximately between the first and third cycle´s height profile.

FC 400:

One sample is tested at FC 400 condition. It shows a smaller recession compared to the FC 200 samples, but a greater one compared to the FC 600 case. The shape does not differ from the other cases.

FC 600:

One sample is tested at FC 600 condition. It shows a smaller recession compared to the FC 200 and FC 400 cases. The shape does not differ from the other cases.

The following observations can be made from these results:

The third cycling test at FC 200 (P50-4 FC 200 Post 3) closely matches the single tests at FC 200 (P50-1 FC 200 & P50-3 FC 200). As the cycle tests were run 3 times 1/3 of the single run test time, thus having the same total test time, it can be concluded that the cycling does not affect the recession, but rather total exposure time.

It is interesting to note that the second cycle run result with the FC 200 condition closely matches the single test with FC 600. The test duration for FC 200 was 60s for each cycle, resulting in an integral heat load for the second cycle of $2 \cdot 200 \frac{kW}{m^2} \cdot 60s = 24000 \frac{kJ}{m^2}$, whereas the integral heat load of the FC 600 is $600 \frac{kW}{m^2} \cdot 60s = 36000 \frac{kJ}{m^2}$. Hence, the exposure time seems to have a greater influence on the recession than the heat flux as even though the integral heat load was increased with the FC 600 case, the recession rate equals the recession rate of the second cycling test.

This is supported by the test with FC 400 where the integral heat load equals the FC 600 case ($400 \frac{kW}{m^2} \cdot 90s = 36000 \frac{kJ}{m^2}$). However, as the exposure time is larger the recession is larger in the FC 400 case than in the FC 600 case. The FC 200 single test case with the same integral heat load ($200 \frac{kW}{m^2} \cdot 180s = 36000 \frac{kJ}{m^2}$) shows the largest recession.

It shall be noted that this statement can, of course, not be extrapolated arbitrarily, as in the limit infinitely large exposure times and heat loads which go to zero would not lead to any recession.

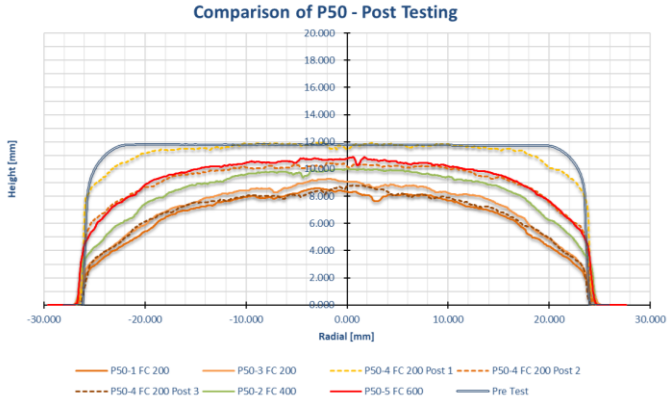

Figure 12: Surface recession of P50 cork

Table 5: P50 - Integral Design Heat Loads

Test id. / Sample	Flow condition	Measured Cold Wall Heat Flux [kW/m²]	Test Duration [s]	Design Heat Load [MJ/m²]	Corrected Design Heat Load° [MJ/m²]
P50-1	FC 200	224	180	36	40.3
P50-2	FC 400	405	90	36	36.5
P50-3	FC 200	224	180	36	40.3
P50-4 A, B, C	FC 200	224	3*60	3*12=36	3*13.4=40.3
P50-5	FC 600	602	60	36	36.1

° Based on the measured cold wall heat flux

Figure 13 below shows the surface height for all TPS05 test results. The blue thin double line shows the pre-test shape. The other lines are color graded depending on their heat fluxes (Orange – FC 200, Green – FC 400, Red – FC 600). The dashed lines show the results for the cycle tests.

First, it shall be noted that the final results show an increase of surface height in the central part and recession only on the sides of the samples. Comparing Figure 13 and Figure 12 in general, shows that the surface of the TPS05 samples remains much smoother after testing than examined for the P50 samples.

FC 200:

In total, three samples are tested at the FC 200 condition (2 instrumented, 1 cycle). However, no usable (absolute) height information for this comparison could be extracted from the sample TPS05-1, thus it is not shown in the diagram. The final height of the two shown FC 200 conditions is not close together, as opposed to the P50 results; the cycle results exhibit a smaller height increase. Taking a closer look at the cycle test outcomes, it can be seen that TPS05-4 results exhibit a dent in the central part, with the highest points being just before the drop off at the edge. Together with the smaller increase to the non-cycle test, one may assume that the entered heat into the probe is smaller during the cycle tests – especially in the inner, protected central part –, thus causing a smaller volume increase.

FC 400:

In total, two samples are tested at the FC 400 condition (1 instrumented, 1 cycle). The final height of those is not close together, as mentions for the FC 200 condition already. Taking a closer look at the cycle test outcomes, it can be seen that TPS05-5 Post 1 and -Post 2 are the only lines that are below the original shape. The discrepancy between the left and right-side results in a piece of cork material that came off during the second cycle. Nevertheless, the left side of those lines appears unaffected by this deviation and shows the pure recession part. As was noticed and described for the FC 200 cycle results, a dent in towards the center is also visible. However, right inside the center, a small increase can be seen. This still fits the previous assumption, since more heat likely entered the sample close to it, due to the surface defect going to a deeper level, causing this local increase.

FC 600:

Only one sample is exposed to the highest heat load condition. It has the smallest increase of surface height, but shows visibly larger recession on the sides. The top surface is level.

Comparing all test cases together the following observations can be made:

As for the tests with P50 the integral heat load was kept constant for all tests with a single run (no cycling). Here comparing FC 200, FC 400 and FC 600, one can observe that, the larger the heat flux is, the smaller is the observable volume increase, while keeping the heat load nearly constant.

The cycling tests for F200 lay very close to each other especially for the first two cycles. For the third cycle a recession of the probe with respect to the second cycle can be observed.

The same tendency can be observed for the FC 400 cycle tests. It seems that the exposure time for the first cycle determines the volume increase, while the second and third cycles lead to a recession from the shape after the first cycle.

Hence, in general it can be stated that the exposure time and the heat flux play a major role for the volume increase of the material. Interrupting the exposure time by cycling, leads to smaller volume increases as the exposure time of the first cycle is more decisive for these increases. In further cycles a recession of the increase volume can be observed.

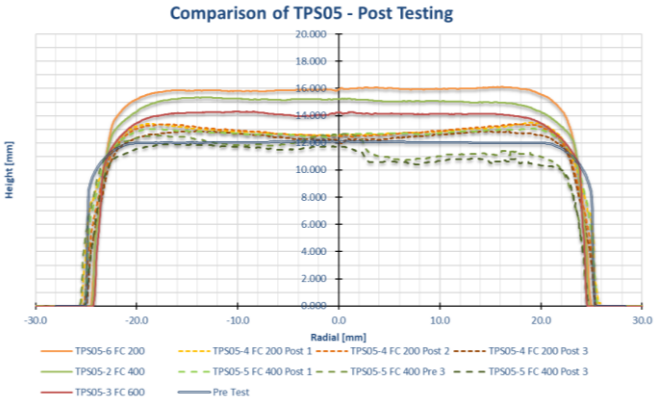

Figure 13: Surface recession of TPS05 cork (gain of volume)

Table 6: TPS05 - Integral Design Heat Loads

Test id. / Sample	Flow condition	Measured Cold Wall Heat Flux [kW/m²]	Test Duration [s]	Design Heat Load [MJ/m²]	Corrected Design Heat Load° [MJ/m²]
TPS05-1	FC 200	224	180	36	40.3
TPS05-2	FC 400	405	90	36	36.5
TPS05-3	FC 600	602	60	36	36.1
TPS05-4 A, B, C	FC 200	224	3*60	3*12=36	3*13.4=40.3
TPS05-5 A, B, C	FC 400	405	3*30	3*12=36	3*12.1=36.5
TPS05-6	FC 200	224	180	36	40.3

° Based on the measured cold wall heat flux

8.2. Weight Change – Cork

As stated in the section of 5.3 Weight Measurements, the mass was measured via a scale with an accuracy of a milligram and a tolerance of ± 5 milligram.

All cork results exhibit a mass decrease, whereas the magnitude is dependent on the test time and heat flux level.

Figure 14 below shows the mass change for all P50 test results. The bars are color graded depending on their heat fluxes (Orange – FC 200, Green – FC 400, Red – FC 600). The shaded bars show the results for the cycle tests. The original sample weight is 31.18 gram on average, ±1.17 gram.

FC 200:

In total, three samples are tested at the FC 200 condition (2 instrumented, 1 cycle). The mass for the non-cycle tests is relatively close together, the final cycle mass loss is lower however. This is an interesting finding, since the recessions was pretty close for those three. A shorter test time resulted in a smaller recession.

Taking a closer look at the cycle test outcomes, the first cycle had the highest mass loss (3.2 g), whereas the following two have a similar but smaller loss (2.3 & 2.2 g).

FC 400:

One sample is tested at FC 400 condition. It shows a smaller mass loss compared to the FC 200 results, but is still nearly the same as the FC 200 cycle final result.

FC 600:

One sample is tested at FC 600 condition. It shows the smallest final weight loss.

These results are coherent with the results presented in section 8.1 on the recession. Here it was stated that for equal integral heat loads the exposure time is presumably more decisive for the recession than the heat load. In the masses one can see the same trend, that for the samples exposed the longest which were the FC 200 cases and which showed most recession also the largest mass loss is observable.

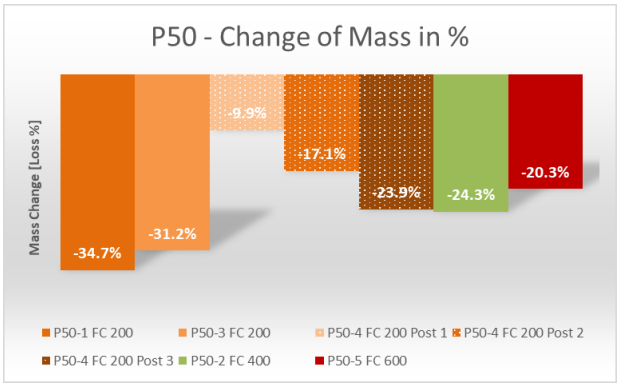

Figure 14: Mass change of cork P50

Figure 15 below shows the mass change for all TPS05 test results. The bars are color graded depending on their heat fluxes (Orange – FC 200, Green – FC 400, Red – FC 600). The shaded bars show the results for the cycle tests. The original sample weight is 45.18 gram on average, ±0.25 gram.

FC 200:

In total, three samples are tested at the FC 200 condition (2 instrumented, 1 cycle). The mass for the non-cycle tests is relatively close together, the final mass for the cycle outcome is lower however. This is an interesting finding, since the height change (remember the mentioned increase) for the cycle outcome was also much smaller.

Taking a closer look at the cycle test outcomes, the first cycle had the highest mass loss (3.6 g), whereas the following two have a similar but smaller loss (1.6 & 1.2 g). The final cycle outcome stays below the non-cycle mass losses.

FC 400:

In total, two samples are tested at the FC 400 condition (1 instrumented, 1 cycle). The mass loss for the instrumented sample is greater compared to the cycle outcomes of the same flow condition. The mass loss of the instrumented sample is smaller compared to FC 200, but larger compared to FC 600, which also fits the findings of the height change, where it was also between the other results.

Taking a closer look at the cycle test outcomes, the first cycle had the highest mass loss (3.2 g), the second a smaller one (2.1 g) and the last cycle showed the smallest weight change (1.5 g). The final cycle outcome stays below the non-cycle mass loss.

FC 600:

One sample is tested at FC 600 condition. It shows the smallest final weight loss.

Interestingly to note is that the FC 200 cycle tests show only a minor shape change compared to the overall picture, but still feature a noticeable and important mass change. For the FC 400 cycle results it needs to be remembered, that a piece of the sample (~0.37 g) broke off during the second run and was removed for the third run. The effect on the height change is greater compared to the effect on the mass change.

Comparing Figure 14 and Figure 15 it is interesting to note that the mass losses between P50 and TPS05 are very comparable even though the shape change discussed in section 8.1 Recession showed to be very different between these two TPS materials.

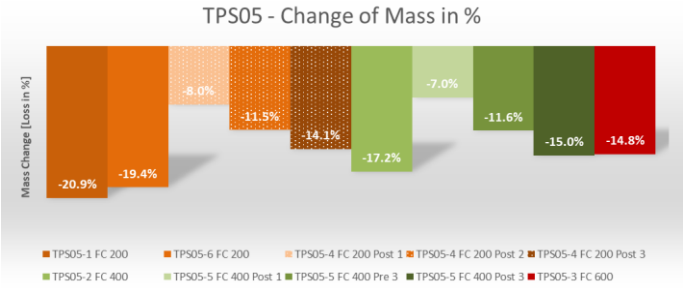

Figure 15: Mass change of Cork TPS05

8.3. Temperature measurements – Cork

For the P50 cork material, no special observations were made regarding the temperature profiles. For the TPS05 cork material, some temperature readings showed minor discontinuities in the form of small temperature drops. No conclusions could be made up to this point. Hence, evaluation of the temperature is subject to further investigations.

8.4. Ceramics

The 3YSZ-10vol.%MWCNTs ceramic samples were found not to be completely heat resistant in its provided composition. During the only wind tunnel test, thin fractured sheets of the ceramic came off at the beginning of the test. A second test in an oven with 1000° Celsius also caused the material to separate, this time in the middle.

For the ZrB_2-40vol.%HfB_2-20vol.%SiC ceramics, no relevant surface recession or change in mass (<0.1%) was found. The surface color of the sample changed a bit and appeared to have a greyish finish.

The Ti_3AlC_2 experienced a small weight increase of about 0.18% (0.13 g) for the FC 800 condition. For FC 600, the increase was about 0.07% (0.055 g) and for FC 200 the increase was the tolerance of the scale. The FC 800 mass increase can also be seen as an increase of surface height, see also Figure 16 for a profile scan. However, this is hardly the case for the FC 600 test, as can be seen in Figure 17.

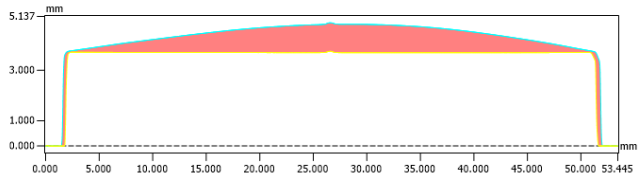

Figure 16: Ti_3AlC_2 – Profile after FC 800

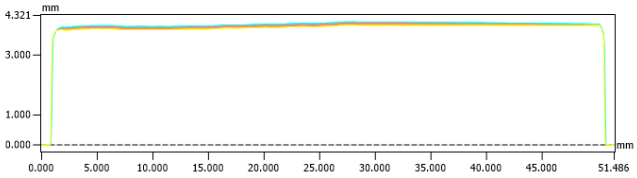

Figure 17: Ti_3AlC_2 – Profile after FC 600

9. SUMMARY & OUTLOOK

In the frame of the RETALT project, cork materials as ablator TPS have been tested in the arc-heated facility of DLR in Cologne at high cold wall heat fluxes. The thermal assessment tests are based on the RETALT1 trajectory and the correspondingly expected heat loads.

Thermal cycle tests have been performed to further investigate the reusability of the cork materials. Additionally, 3 ceramic materials were also tested as a cooperation with the LightCoce project.

It was found, that the cork ablator P50 experiences a mass loss and surface recession based on the heat load and exposure time. Furthermore, it was observed, that the exposure time seems to have a greater impact on the recession in comparison to the heat flux.

The trowelable cork ablator TPS05 experiences a mass loss, surface recession at the outer rim where the shear forces are higher, but it also shows a surface height increase in the central part of the sample. This volume increase is dependent on the heat flux and on the test time, which is highest for the lowest flow condition. Higher heat fluxes, but with a shorter test time, show a smaller increase of volume. Furthermore, the cycle tests diminish this increase greatly, which also seems to be most dependent on the first exposure cycle.

For the ceramics, the 3YSZ-10vol.%MWCNTs samples indicated a low heat resistance, ZrB_2-40vol.%HfB_2-20vol.%SiC showed no change in mass or recession and Ti_3AlC_2 showed a small mass and volume increase, especially for the highest heat flux test.

Further insight in the material behavior is expected to be generated by a more thorough analysis of the temperatures measured with the thermocouples in the future.

10. ACKNOWLEDGEMENTS

The RETALT project has received funding from the European Union's Horizon 2020 research and innovation framework program under grant agreement No 821890.

The LightCoce project has received funding from the European Union's Horizon 2020 research and innovation framework program under grant agreement No. 814632.

The authors also want to express their gratitude to the L2K team. Without their effort, expertise and passion quiring the data presented in this paper would not have been possible.

REFERENCES

[1] Marwege, A.; Klevanski, J.; Hantz, C.; Kirchheck, D.; Gülhan, A.; Karl, S.; Laureti, M.; De Zaiacomo, G.; Vos, J.; Thies, C.; Jevons, M.; Krammer, A.; Lichtenberger, M.; Carvalho, J.; Paixão, S.: „Key Technologies for Retro Propulsive Vertical Descent and Landing – RETALT – an Overview", *2nd FAR conference*, 19–23 June 2022, Heilbronn, Germany.

[2] Maria Wiśniewska, Alex Sullivan, Luca Celotti, Dariusz Garbiec, "Spark Plasma Sintering Of Ceramic-Based Materials For Application In Hypersonic And Re-Entry Vehicles", *2nd FAR conference*, 19–23 June 2022, Heilbronn, Germany.

[3] A. Gülhan and B. Esser, „Arc-Heated Facilities as a Tool to Study Aerothermodynamics Problems of Reentry Vehicles," in *Advanced Hypersonic Test Facilities, Progress in Astronautics and Aeronautics*, Bd. 198, Renton, VA, USA, AIAA, 2002, pp. 375-403.

[4] A. Gülhan, B. Esser, U. Koch, M. Fischer, M. Eggert and V. Hannemann, „Characterization of High-Enthalpy-Flow Environment for Ablation Material Tests Using Advanced Diagnostics," *AIAA Journal*, Bd. 56, Nr. 3, pp. 1072-1084, 2018.

[5] B. Esser and A. Gülhan, „Characterization of new high heat flux test conditions in L," in *7th European Workshop on Thermal Protection Systems and Hot Structures*, Noordwijk, Netherlands, 2013.

[6] M. Laureti, S. Karl, A. Marwege and A. Gulhan, "Aerothermal Databases and CFD based load predictions", *2nd FAR conference*, 19–23 June 2022, https://zenodo.org/record/6592386